

Supporting Information

Water Dissociation and Further Hydroxylation of Perfect and Defective Polar ZnO Model-Surfaces

Mathilde Iachella,¹ Jérémy Cure,² Mehdi Djafari Rouhani,¹ Yves Chabal,² Carole Rossi,¹
Alain Estève^{1,*}

¹University of Toulouse, LAAS-CNRS, 7 avenue du colonel Roche, 31031 Toulouse, France

²Department of Materials Science & Engineering, The University of Texas at Dallas,
Richardson, Texas 75080, United States

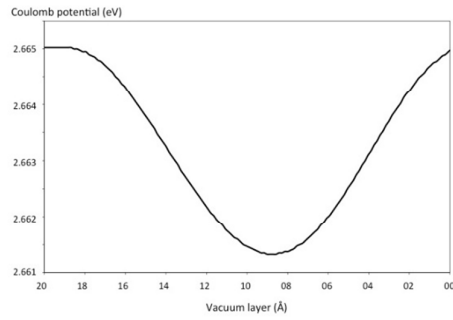
Adsorption energies convergence versus technical choices

In the following (**Table S1**), we have checked the accuracy of our model within different technical choices: (i) with terminal hydrogen atoms on the bottom oxygen layer to compensate the slab overpolarity and fix mobile charges at the bottom of the slab, (ii) using BEEF-vdW functional in order to treat dispersion effects on the adsorption, (iii-iv) energy convergence when varying vacuum thickness, (iii, 25 Å and iv, 15 Å). We observe that terminal hydrogen do not modify the qualitative adsorption results, while quantitatively inducing a ~ 0.1 eV shift on all tested configurations. VdW correction have marginal effects. Finally, convergence is assumed at 20 Å vacuum thickness, which is not the case for 15 Å vacuum.

Table S1. Adsorption energies (eV) on three different configurations and technical treatments, for molecular water, neighboring and far apart H and OH species on p-Zn: with our model, (i) with terminal hydrogen atoms at the slab bottom, (ii) using BEEF-vdW functional in order to treat dispersion effects on the adsorption, (ii-iv) varying the vacuum thickness for energy convergence purpose.

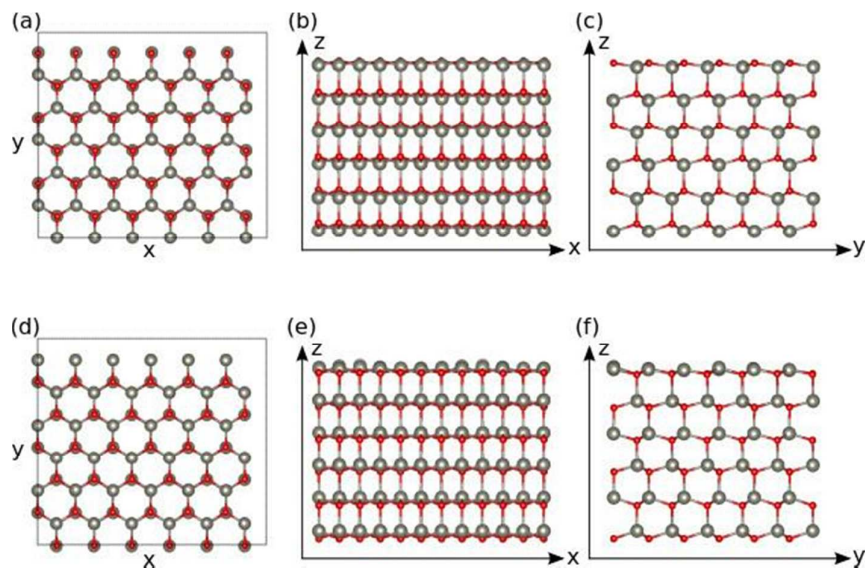
E_{ads} (eV)	H ₂ O/p-Zn	(H+OH)/p-Zn	
		Neighbours	At infinite distance
Our model	-0.48	-1.63	-1.80
Terminal H (i)	-0.35	-1.49	-1.70
BEEF-vdW (ii)	-0.51	-1.65	-1.76
Vacuum 25 Å (iii)	-0.48	-1.64	-1.78
Vacuum 15 Å (iv)	-0.36	-1.72	-1.81

Figure S1. Representation of the electrostatic Coulomb potential with dipole correction in the vacuum layer of p-Zn model surface. Values are taken in the middle of the unit-cell, in the normal axis to the surface, along the vacuum space. We observe that the potential is converged in the order of 10^{-3} eV in the whole vacuum region.



Model surfaces

Figure S2. Representation of the perfect ZnO surfaces considered after geometry optimization. (a-c) correspond to the perfect O-terminated $(000\bar{1})$ surface called p-O. (a) is a top view of the surface, (b) and (c) are side representations considering xz and yz planes, respectively. (d-f) correspond to the perfect Zn-terminated (0001) surface, namely p-Zn. (d) is a top view of the surface, (e) and (f) are side representations considering xz and yz planes, respectively. O atoms are depicted in red, Zn atoms in grey. The $c(6 \times 3)$ supercell used for the calculations is represented as a grey rectangle in (a) and (d). Slabs are 6-layers thick in all the calculations.



The surfaces are built from ZnO slabs containing six full ZnO layers with a $19.8 \times 17.1 \text{ \AA}^2$ surface area and composed of either 36 zinc or 36 oxygen atoms depending on the particular cleavage plane.

In the p-O surface (presented in **Figure 1 a** of the manuscript), the oxygen surface layer just sits slightly above the Zn layer (0.3 \AA interlayer distance). The surface is characterized by three-fold coordinated O atoms and four-fold coordinated sublayer Zn atoms. The top Zn layer of the p-Zn surface sits a little higher above the oxygen sublayer (0.4 \AA interlayer distance); the p-Zn surface is characterized by three-fold coordinated Zn atoms and four-fold coordinated O atoms (**Figure 1 b** of the manuscript).

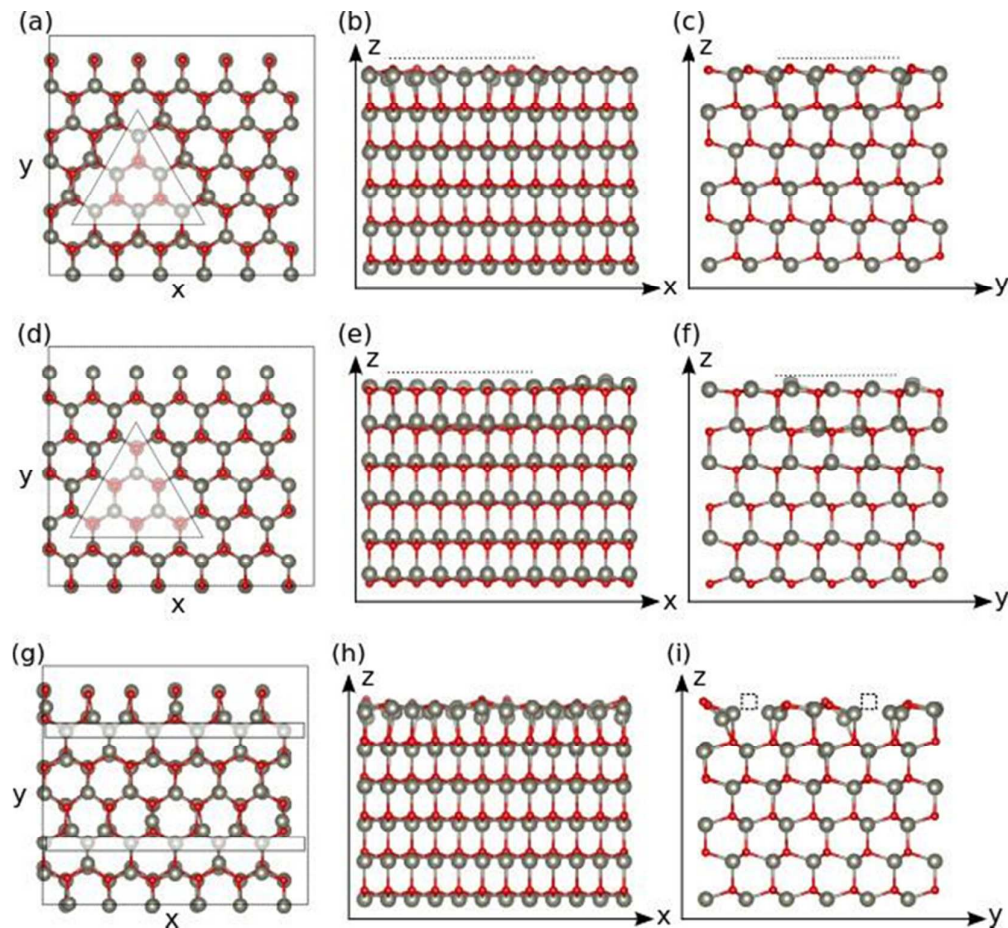


Figure S3. The triangular pit defected p-O ($000\bar{1}$) surface (t-O), presented in (a-c), has a pit defect of 3 Zn and 6 O atoms in the triangle. (a) is a top view of the surface, (b) and (c) are side representations considering xz and yz planes, respectively. The same defect can be created in the (0001) surface (t-Zn) (d-f) with 6 and 3 missing Zn and O atoms, respectively. (d) is a top view of the surface, (e) and (f) are side representations considering xz and yz planes, respectively. In the last defective ($000\bar{1}$) surface shows missing-O rows (r-O), as depicted in (g-i). (g) is a top view of the surface, (h) and (i) are side representations considering xz and yz planes, respectively. O atoms are depicted in red and Zn atoms in grey. The $c(6 \times 3)$ supercell used for the calculations is represented as a grey rectangle in (a), (d) and (g). The different types of vacancies are evidenced by transparent white triangles ((a) and (d)) and rectangles (g) and their positions with dashed lines in (b-c), (e-f) and (i). Slabs are 6-layers thick in all the calculations.).

Defects formation energy

In order to evaluate the surface defects formation energy (E_{form}) for the different ZnO surfaces presented in **Figure 2** of the manuscript, we use the following formula:

$$E_{\text{form}} = E(\text{slab})^{\text{def}} + N_{\text{O}} E(\text{O}/\text{ZnO}) + N_{\text{Zn}} E(\text{Zn}/\text{ZnO}) - (N_{\text{O}} + N_{\text{Zn}} + 1) E(\text{slab})^{\text{perf}} \quad (\text{S1})$$

Where $E(\text{slab})^{\text{perf}}$ is the total energy of the perfect ZnO slab, N_{O} and N_{Zn} are the numbers of oxygen and zinc vacancies in the defective slab, $E(\text{O}/\text{ZnO})$ and $E(\text{Zn}/\text{ZnO})$ are the energies of the adsorbed oxygen and zinc atoms at an infinite distance from the default, respectively. We thus define the area normalized defect formation energy $E_{\text{form}}^{\text{A}}$ as follows:

$$E_{\text{form}}^{\text{A}} = E_{\text{form}} / A \quad (\text{S2})$$

With A , the area of the considered slab (in \AA^2). In **Table S2** those different energies are presented for the different defective t-O (see **Figure S3** a-c), t-Zn (**Figure S3** d-f) and r-O (**Figure S3** g-i) ZnO surfaces. All these energies are positive. The defect formation energy of the triangular pit t-O and t-Zn surfaces are almost similar (+0.06 vs +0.01 eV, respectively,

see **Table S2**). The formation energy of missing oxygen rows in the (0001) surface is in the range of the t-O value, 0.05 eV. The ADC reconstruction is a highly defective surface compared to its t-Zn basis, that necessitates 0.04 eV.

Table S2. Number of Zn (N_{Zn}) and oxygen vacancies (N_{O}) in the different defective surfaces used: triangular pit defected p-O (000 $\bar{1}$) surface (t-O), triangular pit defected p-Zn (0001) surface (t-Zn), missing-O rows O-terminated (000 $\bar{1}$) surface (r-O). The normalized formation energy ($E_{\text{form}}^{\text{A}}$, eV. \AA^{-2}) of those vacancies at 0 K has been evaluated. The different surfaces are depicted in **Figure 2** of the manuscript, except for the ADC reconstruction that can be viewed in Ref. [26].

Surface	N_{Zn}	N_{O}	$E_{\text{form}}^{\text{A}}$ (eV. \AA^{-2})
t-O	3	6	0.06
t-Zn	6	3	0.01
r-O	0	12	0.05
ADC reconstruction	18	9	0.04

Water molecular adsorption

We have studied the water molecular adsorption on the different ZnO surfaces (p-O, p-Zn, t-O, t-Zn and r-O, depicted in **Figures 1** and **2** of the main text) considering all non-reducible adsorption sites. **Table S3** exposes the corresponding local minima after geometric optimization, and their molecular adsorption energies. In addition, on p-O, an additional site has been tested for adsorbing the water molecule: the single oxygen vacancy. It appears that the adsorption energy is more stabilizing than on the other adsorption sites on the very same surface (-0.84 eV vs -0.21 eV for the most stable adsorption site on the non-defective surface).

On p-Zn, only two configurations are found as local minima for water molecule adsorption: the top site on a zinc atom and the six fold coordinated hollow site. On the defective surfaces, many non-reducible adsorption sites have been tested. Regarding both t-O and t-Zn, four different zones have been considered: the terrace surface, close to p-O and p-Zn; the vertex (adsorption in the angle of the triangle); the step edges of the triangle, namely edge sites; and the bottom of the well called pit in **Table S3**. On both surfaces, the pit better traps the water molecule. At last, on the r-O defective surface, the best adsorption energies correspond to the cases where water molecules fill a surface defect (-1.13 eV on the bridge Zn^e-O^e site and -0.90 eV on the top site of a zinc atom behind the missing row).

Table S3. Local minima found for the adsorption of water molecules on each ZnO model-surfaces: p-O, p-, t-O, t-Zn (, and r-O. The molecular adsorption energy of water (ΔE_{ads}^{mol} , eV) has been calculated for each surface, and reported in this Table. The letters in exponent of an atom depicts its position in the structure: in the terrace (t), edge (e) or pit (p).

Surface		Site	ΔE_{ads}^{mol} (eV)
p-O		Top O ^t	-0.02
		Top Zn ^t	-0.21
		Hollow	-0.12
		Vacancy	-0.84
p-Zn		Top Zn ^t	-0.48
		Hollow	-0.26
t-O	Terrace	Top O ^t	-0.02
		Top Zn ^t	-0.21
		Hollow	-0.13
t-O	Vertex	Top O ^e	-0.21
		Top Zn ^v	-0.21
		Bridge Zn ^v O ^e	-0.18
		Hollow	-0.15
t-O	Edge	Top O ^e	-0.16
		Top Zn ^e	-0.40
		Bridge Zn ^e O ^e	-0.45
		Hollow	-0.11
t-O	Pit	Top Zn ^p	-0.76
t-Zn	Terrace	Top Zn ^t	-0.43
		Hollow	-0.07
t-Zn	Vertex	Top O ^v	-0.08

		Top Zn ^e	-0.28
		Bridge Zn ^e O ^v	-0.43
		Hollow	-0.13
t-Zn	Edge	Top Zn ^e	-0.24
		Bridge Zn ^e O ^e	-0.35
		Hollow	-0.06
t-Zn	Pit	Top Zn ^p	-1.10
r-O		Top O ^e	-0.29
		Bridge Zn ^e -O ^e	Dissociation
		Top Zn ^t	-0.41
		Top Zn ^p	Dissociation
		Bridge Zn ^t O ^e	-0.44
		Hollow	-0.29

We have first studied the adsorption of water on a single oxygen vacancy created on p-O. This adsorption site leads to a strong stabilization energy of -0.85 eV (see **Table 1**), making water adsorption almost twice more stable than on both perfect surfaces. The water molecule adsorbs on the vacancy sites with the hydrogen atoms pointing towards the outer surface. The corresponding structure is depicted in **Figure S4** a and b.

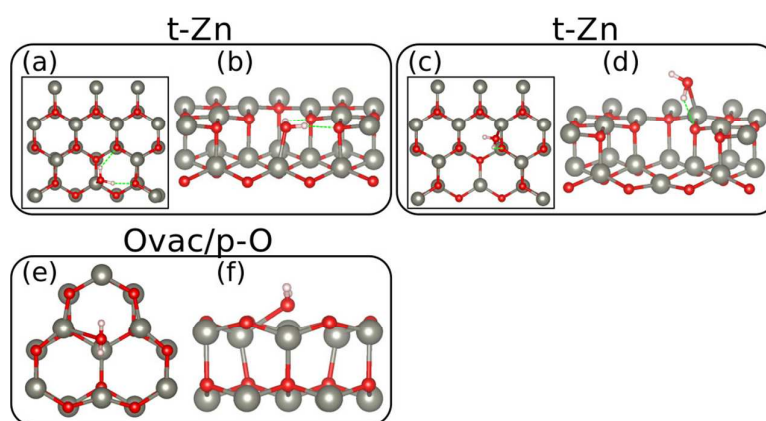


Figure S4. Representation of the adsorption structures of a water molecule on t-Zn (a-d) p-O with single oxygen vacancy (e-f) and surfaces. (a), (c) and (e) are reduced top views of the adsorption structures; (b), (d) and (f) are reduced side views. O atoms are depicted in red, Zn atoms in grey and H atoms in white. Hydrogen bonds are represented with a green dashed line.

On the other t-O sites, namely *e* and *p*, water adsorption is, energetically, more than two times less favourable, with adsorption energies between -0.02 and -0.45 eV (see **Table S3**). Note that the latter adsorption in the pit configuration shows a higher adsorption energy of -0.45 eV, compared to the similar local configuration on p-O (-0.21 eV). This is due to the filling of an oxygen vacancy, which has been evidenced to be stabilizing.

Water dissociative adsorption

We have studied the water dissociative adsorption on the different ZnO surfaces (p-O, p-Zn, t-O, t-Zn and r-O, depicted in **Figures 1** and **2**) starting from the global minima structures of the molecular adsorption on each support. Hydroxyl, that is the heaviest group in water dissociation, has been considered fixed at the former water adsorption site as a starting point, and all proton positions have been tested around. **Table S4** exposes the corresponding local minima after geometric optimization, their adsorption and dissociation energies.

On both perfect supports, the proton leaves the water molecule to join the next under coordinated atom (Zn for p-Zn surface, O for p-O). In those cases, the only exothermic dissociation process happens on p-Zn. On t-O, wherever the proton binds, the cases have similar energy profiles, with a dissociation energy in the range -0.85 -0.91 eV. On t-Zn, the calculations have led to only exothermic dissociation energies (from +0.99 to +1.86 eV). To find a case where the dissociation is favourable, we have performed the same dissociative adsorption process using the second most stable molecular adsorption site. Indeed, we have found two local minima, one of them being as favourable on this support as the molecular adsorption (dissociative adsorption of -1.10 eV). On r-O, all local minima were isoenergetic (with a dissociative adsorption energy of -2.68 eV), and the proton has diffused towards an oxygen atom.

Table S4. Local minima found for the dissociative adsorption of water molecules on each ZnO model-surfaces: p-O, p-Zn, t-O, t-Zn and r-O. The molecular adsorption energy of water (ΔE_{ads}^{mol} , eV) has been recalled for each surface. The dissociation energy (ΔE_{diss} , eV) and dissociative adsorption energy (ΔE_{ads}^{diss} , eV) have been calculated and reported in this Table. The letters in exponent of an atom depict its position in the structure: in the terrace (t), edge (e), or pit (p) of the surface.

Surface	Site OH	Site H	ΔE_{ads}^{mol}	ΔE_{diss}	ΔE_{ads}^{diss}
p-O	Top Zn ^t	Top Zn ^t	+0.46	-0.21	+0.67
	Top Zn ^t	Top O ^t	+0.15	-0.21	+0.37
O _{vac} /p-O	Top Vacancy	Top Zn ^t	-2.33	-1.48	-0.85
p-Zn	Bridge Zn ^t Zn ^t	Top Zn ^t	-1.28	-0.48	-0.80
	Bridge Zn ^t Zn ^t	Top O ^t	-0.08	-0.48	+0.40
t-O	Top Zn ^p	Top O ^p	-1.70	-0.80	-0.91
	Top Zn ^p	Top O ^e	-1.70	-0.80	-0.90
	Top Zn ^p	Top O ^t	-1.65	-0.80	-0.86
t-Zn	Top Zn ^p	Top Zn ^e	+0.75	-1.10	+1.86
	Top Zn ^p	Top Zn ^p	-0.11	-1.10	+0.99
	Top Zn ^p	Top O ^e	+0.24	-1.10	+1.34
	Top Zn ^e	Top Zn ^e	-0.82	-0.24	-0.58
	Top Zn ^e	Top O ^e	-1.10	-0.24	-0.86
r-O	Bridge Zn ^e -O ^e	Top O ^e	-2.68	-1.14	-1.55

On p-O with an oxygen vacancy, the dissociation energies exhibit favourable trend: -1.48 eV (**Table S4**). The hydroxyl stays at the vacancy location, while the proton links to the neighbouring surface oxygen atom. This structure is presented in **Figure 4** e and f. This result indicates that defects are mandatory on p-O surfaces for promoting dissociation.

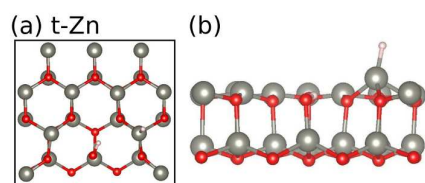


Figure S5. Representation of the adsorption configuration of a dissociated water molecule on t-Zn. (a) is a reduced top view of the adsorption structure, (b) is a reduced side view. O atoms are depicted in red, Zn atoms in grey and H atoms in white.

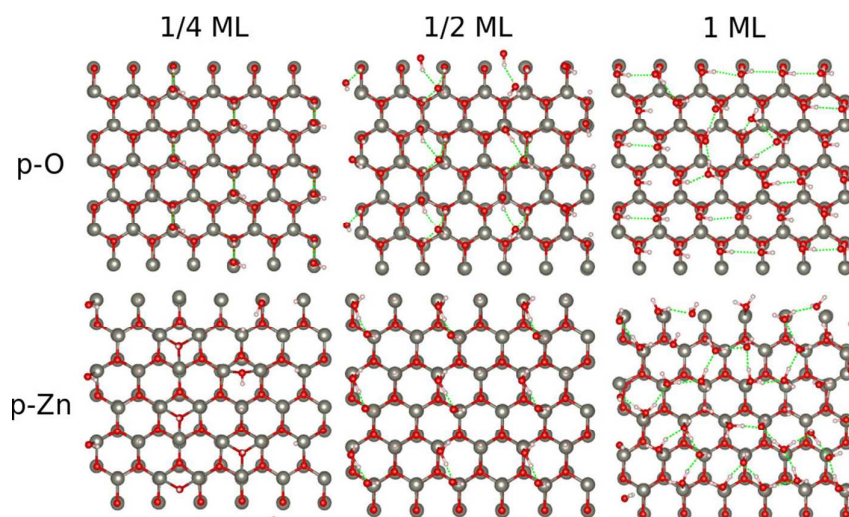


Figure S6. Representation of the adsorption structures of $\frac{1}{4}$, $\frac{1}{2}$ and 1 ML of dissociated water molecules on p-O and p-Zn. O atoms are depicted in red, Zn atoms in grey, H atoms in white and hydrogen bonds in green dashed lines.

In **Figure S6**, the dissociated water molecules adsorption structures have been represented for $\frac{1}{4}$, $\frac{1}{2}$ and 1 ML on both p-O and p-Zn. On p-O, the number of hydrogen bonds is around one per adsorbed molecule, whatever the coverage. Moreover, two water molecules are reassociated in the case of the half monolayer (with 18 molecules in total in the supercell) and 35 in the case of the full ML (with 36 molecules in total in the supercell). Regarding the dissociative adsorption on p-Zn, no hydrogen bonds are formed in the case of $\frac{1}{4}$ ML. When increasing the coverage, one can count around 0.5 hydrogen bond per adsorbed water molecule. On the $\frac{1}{2}$ ML at p-Zn, half of the molecules are re-associated. Finally, on the 1 ML

coverage, 26 water molecules are re-associated (among 36 H+OH on the surface), and two hydrogen molecules are formed.

OH islanding

In **Figure S7 b**, we see that the central OH is in a hollow position, whereas the six surrounding hydroxyl groups are in between Zn-Zn bridging and hollow positions. The associated structures are very similar for both islands. The 7 central OH are in hollow positions and the 12 surrounding hydroxyl species are arranged in between hollow and bridging sites, as shown in **Figure S7 c**.

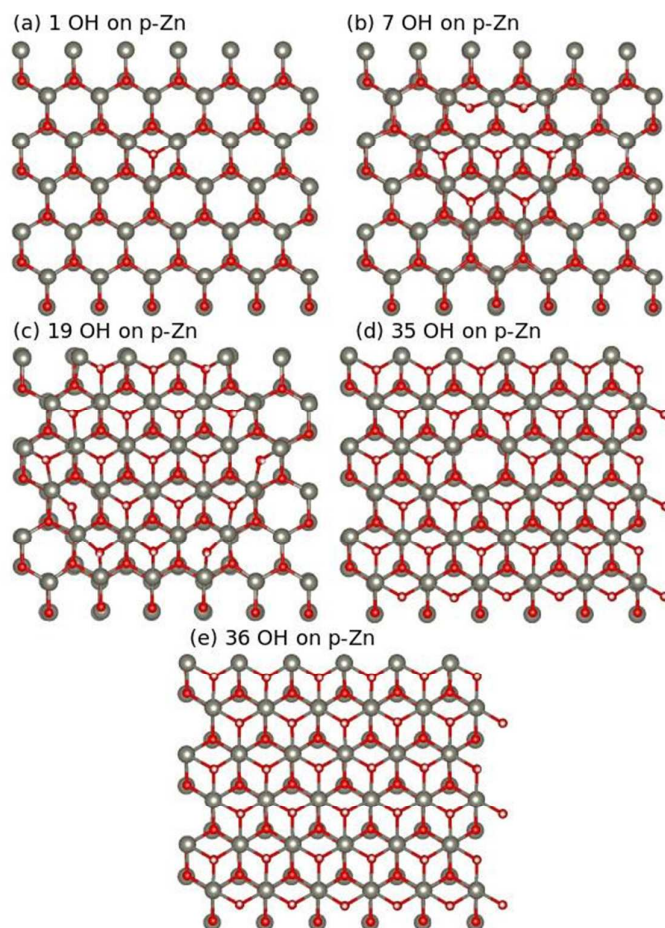


Figure S7. Adsorption structure top views, after minimization, of (a) 1 OH, (b) 7 OH, (c) 19 OH as islands, (d) 35 OH and (e) 1.0 ML (36 OH) of hydroxyl species on p-Zn. O atoms are depicted in red, Zn atoms in grey and H atoms in white.

Discussion relative to ADC reconstruction

In order to check the convergence of our t-Zn defective model referred to the literature, we have performed a set of comparative calculations giving the p(6x6) reconstructed surface model available in Ref. 26, reproduced within our methodology. In **Table S5**, we have tested the adsorption of one to three water molecules as well as dissociative configurations. In addition, we have tested the interaction of a single water molecule at the vertex of the pit, and found barrierless dissociation mechanism, confirming our finding with a different pit defective Zn-face.

Table S5. Adsorption energies (eV) for water on the ADC p(6x6) reconstruction as in Ref. [26], which is reproduced within our methodology, see “our calculations”.

E_{ads} (eV)		Top Zn ^p /---O ^e
Ref. [26]	1 H ₂ O	<i>Not calculated</i>
	2 H ₂ O	-1.49
	H ₂ O+OH+H	-1.51
	3H ₂ O	-1.40
	2H ₂ O+OH+H	-1.48
Our calculations	1 H ₂ O	-1.52
	2 H ₂ O	-1.37
	H ₂ O+OH+H	-1.38
	3H ₂ O	-1.27
	2H ₂ O+OH+H	-1.36

Hydroxyl distribution and coverage

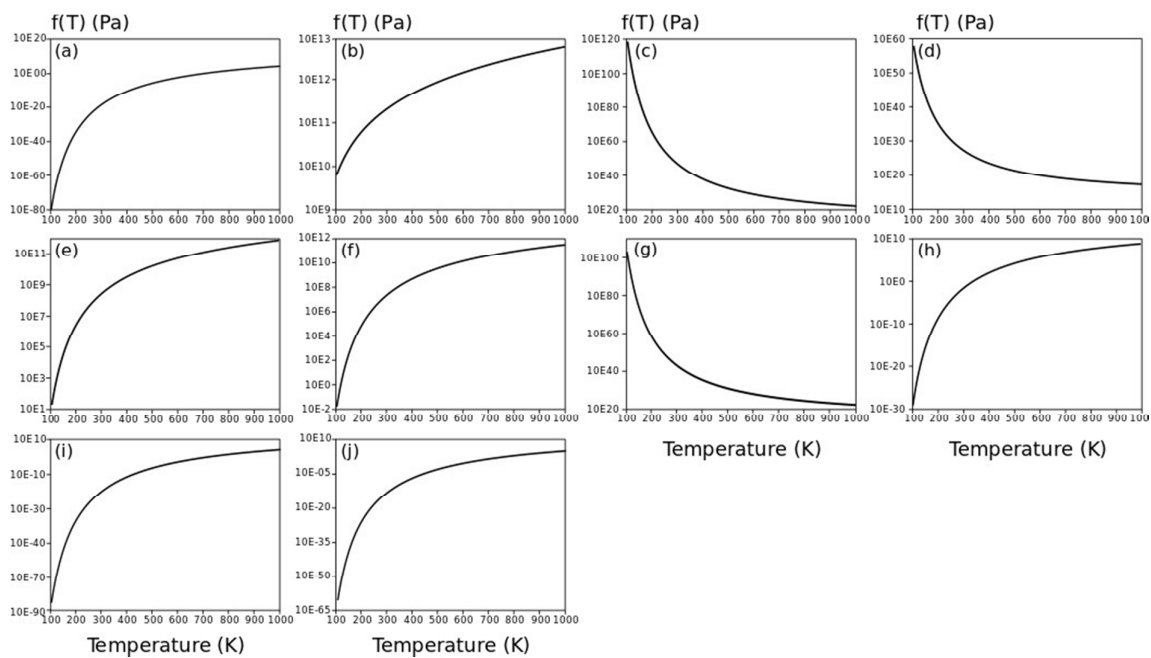


Figure S8. Graphs representing the pressure needed, as a function of temperature, for the adsorption of (a), (e), (i), (j) 1 OH, (b), (f) $1/4$, (c), (g) $1/2$ and (d), (h) 1 ML of dissociated water molecules on (a-d) p-O, (e-h) p-Zn, (i) t-O and (j) t-Zn.